New Reentrant Wetting Phenomena and Critical Behavior near Bulk Critical Points

C. Ebner and W. F. Saam
Department of Physics, The Ohio State University, Columbus, Ohio 43210
(Received 6 November 1986)

Wetting phenomena near the bulk critical point of an adsorbate are examined for the realistic case of long-ranged (e.g., van der Waals) forces, with use of mean-field theory for an Ising lattice-gas system. For moderately strong long-ranged forces new critical behavior appears at and near T_c, accompanied by both reentrant wetting and dewetting transitions and the appearance of two distinct wetting phases.

PACS Numbers: 68.45.Gd, 68.15.+e, 68.35.Md

Current theoretical understanding of wetting phenomena near a bulk critical temperature T_c in real systems, e.g., ones with van der Waals forces, is based in large measure on recent detailed mean-field calculations[1,2] for Ising lattice-gas systems supplemented by some general arguments.[3] The predictions can be understood in the context of earlier work by Nakanishi and Fisher[4] (NF) on the case of short-ranged forces because certain important features survive nearly intact.[1,2] However, as we discuss here, this statement is true only for relatively weak long-ranged forces. For stronger, but still physically reasonable, forces, new transitions appear, some accompanied by striking reentrant wetting (and nonwetting) behavior.

Our results are obtained within mean-field theory (MFT) for an Ising lattice gas. As has been noted elsewhere,[2] the essential features of long-ranged forces are governed by a linear combination of adsorbate-substrate (AS) and adsorbate-adsorbate forces. We therefore simplify our computations by using only a short-ranged adsorbate-adsorbate interaction, regarding our long-ranged AS interaction as an effective interaction incorporating the essential effects of all long-ranged forces. The validity of this procedure in MFT has been checked[2] in selected cases. Our long-ranged AS interaction is taken to vary as z^{-4}, where z is the distance from the substrate, rather than z^{-3}, which would be the behavior of unretarded van der Waals forces, because the latter has a marginal range in MFT in three dimensions. We choose to use a submarginal case in our MFT since the $1/z^3$ potential is submarginal when fluctuations are taken into account, i.e., in the real world.[5] We hence expect our results to be relevant to real systems with van der Waals forces. The marginal case in MFT will be the topic of a separate publication.

In MFT, the free-energy function for our model may be written in magnetic language as

$$\Omega=\sum_{i\geq 1}[(r/2)(m_i-m_{i+1})^2+f(m_i)-h_i m_i]-gm_1-gm_1^2/2\ , \tag{1}$$

in which m_i is the expectation value of a spin in the ith layer from the substrate; in terms of the particle number density ρ_i, $m_i=2\rho_i-1$. If $-\varepsilon_\perp$ is the interaction energy between nearest-neighbor atoms in adjacent layers and $\nu_\perp$ is the number of such neighbors that a site has, then $r=\varepsilon_\perp\nu_\perp/4$. If $\varepsilon_\parallel$ and $\nu_\parallel$ are analogous intralayer quantities, and if the interaction within the first layer is $-\varepsilon_\parallel(1+D)$, then $g=-(\varepsilon_\perp\nu_\perp-\varepsilon_\parallel\nu_\parallel D)/4$. Further, $h_i=-U_i/2$ where U_i is the AS interaction in layer i, and

$$f(m)=\frac{\mu_0 m^2}{4}+T\left[\left(\frac{1+m}{2}\right)\ln\left(\frac{1+m}{2}\right)+\left(\frac{1-m}{2}\right)\ln\left(\frac{1-m}{2}\right)\right]\simeq\frac{tm^2}{2}+\frac{u_0 m^4}{4}+\ldots\ , \tag{2}$$

where $u_0=T/3$; $\mu_0=-(\varepsilon_\perp\nu_\perp+\varepsilon_\parallel\nu_\parallel/2)$ is the chemical potential at bulk coexistence; and $t=T+\mu_0/2=T-T_c$. Minimization of $\Omega(\{m_i\})$ produces the mean-field equations

$$f'(m_i)-r(m_{i+1}-2m_i+m_{i-1})-h_i=0,\quad i\geq 2, \tag{3a}$$

$$f'(m_1)-r(m_2-m_1)-\tilde{h}_1-gm_1=0, \tag{3b}$$

where $\tilde{h}_1=g-U_1/2$.

The case of NF is $h_i=0$, $i>1$. For this case the phase diagrams (cf. Ref. 4) in U_1-t space show lines of wetting and drying transitions at $t<0$ which meet at $t=0$ in an ordinary point (O) if $g<0$, a special point (SP) if $g=0$, or an extraordinary point (E) if $g>0$. These transitions are always first order except in the case of $g<0$ for which they are continuous at small $|t|$ but become first order at tricritical points at some larger value of $|t|$. As $g\to 0$, the tricritical points rise in temperature and merge into the special point at $g=0$. Within MFT the various lines are described at small $|t|$ by $|t|\sim|\tilde{h}_1|^{1/\Delta_1}$ where $\Delta_1=\frac{1}{2}$, 1, and $\frac{3}{2}$ for $g<0$, $g=0$, and $g>0$, respectively.

If there is a long-ranged potential U_i which is not too

large, fairly intuitive qualitative arguments can be used[2] to predict the changes relative to the NF case. Briefly, if $U_n = U/n^x$ for $n > 1$, the free energy of a wetting film of thickness l acquires a piece $\Delta\Omega = A/l^{x-1}$ where $A > 0$ if $U < 0$. This free energy has a minimum at $l = \infty$, and a transition to this state from one with finite l can only occur discontinuously; i.e., it must be a first-order transition. For a drying film, $\Delta\Omega = -A/l^{x-1}$ and, for $t \neq 0$, there is never a minimum at $l = \infty$, i.e., drying transitions cannot take place because the long-range potential traps a film that would otherwise dry. There is, however, a continuous drying transition at $t = 0$ ($T = T_c$). These arguments suggest that the phase diagrams shown in Fig. 1 replace those of NF for long-ranged potentials with g and $\tilde{h}_1$ replaced by effective equivalent parameters. In Fig. 1, W and PD are always lines of first-order wetting and partial drying transitions, the latter being characterized by a finite discontinuity in l. The line PD ends at a critical point for $g^{\text{eff}} < 0$; for all g^{eff} there is drying only at T_c and $h_1^{\text{eff}} < 0$. Detailed mean-field calculations[2] for relatively weak potentials $U_n = U/n^x$, $x \geq 4$, show that Fig. 1 is correct. However, significant changes, including new phase transitions and reentrant wetting and nonwetting, appear for sufficiently strong U.[6] We turn now to discussion of these new phenomena.

We begin with an instructive but brief analytic study of special points; this is best done by our casting the equations in the form of an effectively short-ranged potential problem, a procedure which has been given in more detail elsewhere.[2] We first write $m_n \equiv \tilde{m}_n + \delta m_n$,

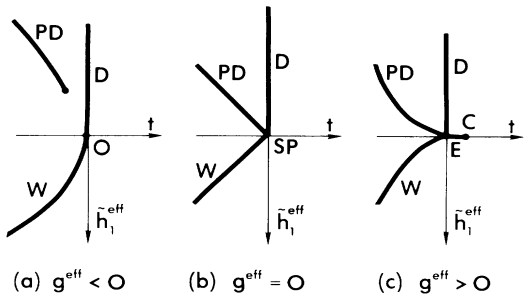

(a) $g^{\text{eff}} < 0$ (b) $g^{\text{eff}} = 0$ (c) $g^{\text{eff}} > 0$

FIG. 1. Phase diagrams in $\tilde{h}_1$-t space for $|U| < U_c$ and for (a) $g^{\text{eff}} < 0$, (b) $g^{\text{eff}} = 0$, (c) $g^{\text{eff}} > 0$. Details are discussed in the text.

where $\tilde{m}_n$ satisfies the homogeneous equation

$$f'(\tilde{m}_n) - r[\tilde{m}_{n+1} + \tilde{m}_{n-1} - 2\tilde{m}_n] = 0. \tag{4}$$

By iterating in from large n where h_n is negligible, we find a surface boundary condition on $\tilde{m}_n$ given by

$$r(\tilde{m}_2 - \tilde{m}_1) = -h_1^{\text{eff}} - g^{\text{eff}}\tilde{m}_1 + u_0\tilde{m}_1^3, \tag{5a}$$

$$h_1^{\text{eff}} = \tilde{h}_1 + g\delta m_1 + r(\delta m_2 - \delta m_1) - u_0\delta m_1^3, \tag{5b}$$

$$g^{\text{eff}} = g - 3u_0[\tilde{m}_1\delta m_1 + \delta m_1^2], \tag{5c}$$

if $f(m)$ is taken as (at $t = 0$) $u_0 m^4/4$. The effective surface field h_1^{eff} and coupling enhancement g^{eff} depend on the δm_n which are given by

$$\delta m_n = (2\delta m_{n+1} - \delta m_{n+2}) - h_n/r + [f'(\tilde{m}_{n+1} + \delta m_{n+1}) - f'(\tilde{m}_{n+1})]/r. \tag{6}$$

At ordinary and special points, $\tilde{m}_n = 0$ if h_n is small enough.[2] Thus one is motivated to look at small values of $\tilde{m}_n$, assuming that the h_n's are not too large. Then Eq. (6) may be approximately solved and one finds in place of Eq. (5a)

$$r(\tilde{m}_2 - \tilde{m}_1) = -\hat{h}_1 - \hat{g}\tilde{m}_1 - 3u_0H_2\tilde{m}_1^2 + u_0\tilde{m}_1^3, \tag{7}$$

where $\hat{h}_1$ and $\hat{g}$ are constants and only the most important quadratic and cubic terms in $\tilde{m}_n$'s are kept while higher-order terms are discarded. Also,

$$\delta m_n \approx -H_{n+1} \equiv -\frac{1}{r}\sum_{l=n}^{\infty}(l - n + 1)h_l. \tag{8}$$

One now solves Eq. (4) subject to the condition Eq. (7). At a special point where $\hat{h}_1 = 0$ and $g = 0$ in the short-ranged case, the only solution is $\tilde{m}_n = 0$. In the long-ranged case, a new solution appears if H_2 is large enough. To see this, note that $m_n = A/(\lambda + n)$ solves Eq. (4) with $A = 0$ or $\pm(2r/u_0)^{1/2}$ if $\lambda \gg 1$. Use of this form of $\tilde{m}_n$ in Eq. (7) yields $\lambda = (u_0A^2/r)(3u_0H_2A/r - 1)^{-1}$. Since we must have $\lambda > 0$ for a physically sensible solution, we must have $A = (2r/u_0)^{1/2}$ and $H_2 > (r/18u_0)^{1/2}$. If we let $U_n = U/n^4$ for $n \geq 2$, then $H_2 = -0.11883U/2r$. For a fcc lattice with a [111] direction normal to the substrate, $\nu_\parallel = 6$ and $\nu_\perp = 3$. Further, taking $\varepsilon_\perp = \varepsilon_\parallel = \frac{1}{3}$ so that $T_c = 1$, we have $\mu_0 = -2$ and $r = \frac{1}{4}$. Using these facts and noting that $u_0(t = 0) = \frac{1}{3}$, we find the approximate criterion for the appearance of a new solution to be, for an attractive potential, $|U| > 0.859 \equiv U_c$.

The stability of this solution is difficult to determine analytically. Numerical solution of the full MFT shows that it first appears for $|U| \simeq 0.7$–0.8, somewhat below the approximate analytic prediction, and that it is the stable solution. More general numerical solution of the mean-field equations at T_c produces the results summarized in Fig. 2. For $|U| < U_c$, the changeover from O to E points as a function of g occurs at a special point as shown in Fig. 2(a). For $|U| > U_c$, the behavior is depicted in Fig. 2(b). The predicted special point SP is not a stable solution; nor are the predicted ordinary points O to the right of the crossover point X. Rather, for any given $g > g_X$ there is always a point E′ where two solutions coexist, as in characteristic of an extraordinary point. As U_1 decreases from this point at constant g, one solution becomes metastable; this is the one that evolves

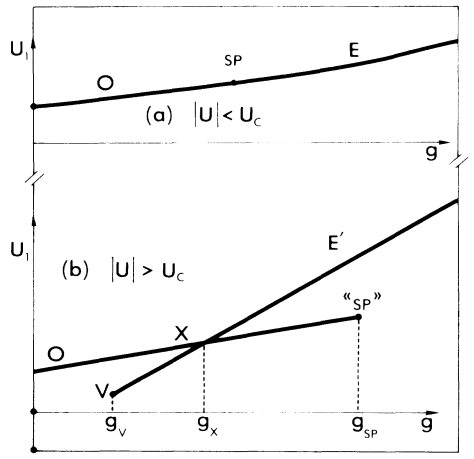

FIG. 2. Phase diagrams in U_1-g space at $t=0$ for (a) $|U|<U_c$ and (b) $|U|>U_c$.

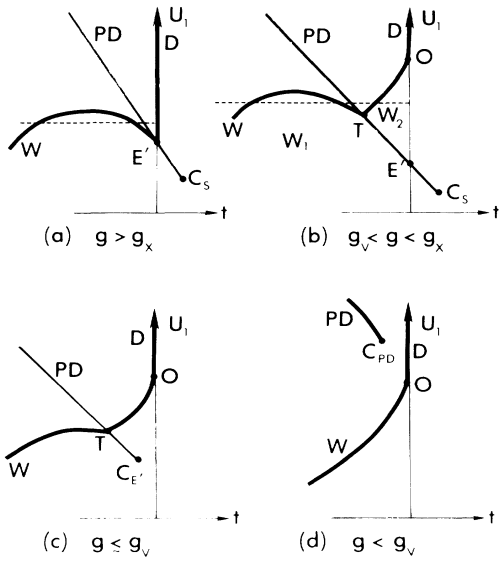

FIG. 3. Phase diagrams in U_1-t space for $|U|>U_c$ and (a) $g>g_X$, (b) $g_V<g<g_X$, (c) g slightly less than g_V, and (d) g significantly smaller than g_V. Details are discussed in the text.

into the ordinary-pointlike solution on the line O, given that $g<g_{SP}$. For $g<g_X$, on the other hand, one has the unexpected occurrence of both a line of stable ordinary points O and a line of stable points E′ which terminates at V. The range of g for which this behavior is found depends on U; at $U=-1.0$, $g_V=0.0445$, $g_X=0.0523$, and $g_{SP}=0.0612$, while for $U=-1.5$ $g_V=0.0680$, $g_X=0.0950$, and $g_{SP}=0.150$; increasing $|U|$ produces a larger interval g_X-g_V.

To understand further the behavior of these systems we consider next the regime $T<T_c$ at bulk coexistence. Figure 3 shows qualitative U_1-t phase diagrams for fixed g as determined by detailed numerical solution of Eqs. (3). Figure 3(a) is for $g>g_X$. Here W and PD are lines of first-order wetting and partial drying transition, and E′C is a line of surface phase transitions. There is complete drying at T_c on line D. This phase diagram should be compared to Fig. 1(c) for $|U|<U_c$; the exponents describing the behavior of W and PD near T_c are clearly different for the two cases so that E′ is not a conventional extraordinary point. Further, notice that if T is increased to T_c along the dashed line in Fig. 3(a), the system goes from nonwetting to wetting to nonwetting (given wetting boundary conditions); that is, there is reentrant nonwetting.

Next, consider the case $g_V<g<g_X$ of Fig. 3(b). There is a line WT of first-order wetting transitions to a wet phase W_1; TE′ is a line of first-order transitions between distinct wet phases W_1 and W_2 which have different density profiles close to the substrate; and TO is a line of first-order wetting transitions to W_2. These are found for wetting boundary conditions; with drying boundary conditions there is a line of first-order partial drying transitions PD, part of which is coincident with the line TE′. There is complete drying only on line D at T_c. The only difference between the film profiles along TE′ for the two kinds of boundary conditions is the presence of the "liquid-vapor" interface far from the substrate in the case of wetting boundary conditions. Finally, there is a line E′C_s of first-order surface transitions. The scale of the figure may be set by some typical numbers. For example $U=-1.5$ and $g=0.08$, O is at $U_1=0.2609$, E′ is at $U_1=0.2529$ and T is at $t=-0.0012$ and $U_1=0.2537$ in MFT.

The points E′ and O have some characteristics of extraordinary and ordinary points. At E′ there are two coexisting phases, and at O there is but one with $\tilde{m}_n=0$. The curve TO is parabolic at O. However, the behavior of TE′ at E′ is different from that near extraordinary points. The crossover from Fig. 3(a) to 3(b) occurs at $g=g_X$ where O crosses E′ and becomes stable [cf. Fig. 2(b)]. The point X is a previously unknown type of critical point. The behavior of the wetting films for the case of Fig. 3(b) is truly remarkable; if the temperature is increased so that the system follows the dashed line up to T_c, there will be both reentrant wetting and reentrant nonwetting.

As g is decreased toward g_V, the point C_s approaches E′, reaching it when $g=g_V$. For slightly smaller g, E′ is gone and one has the phase diagram of Fig. 3(c) with an Ising-like critical point $C_{E'}$. Further reduction of G causes $C_{E'}$ to move across T so that this triple point is gone; Fig. 3(d), which is essentially the same as Fig. 1(a), then emerges and persists as g is decreased.

We briefly summarize the essential characteristics of the potentials for which the above new phenomena are found. Specifically, to produce E′ points there are three requirements: (1) The effective long-ranged potential must be strong ($|U|\sim 1$) and favor wetting, (2) the

first-layer coupling must be considerably enhanced ($D \gtrsim \frac{1}{2}$; i.e., $g \gtrsim 0$), and (3) the first-layer field U_1 must be repulsive ($U_1 \sim +2g$). The latter two requirements are necessary for E points in the more conventional case[1,2] of Fig. 1. For a repulsive effective long-range potential there are analogous phenomena when wetting and drying boundary conditions far from the substrate are interchanged.

The results presented here make it abundantly clear that to assume that calculated wetting phenomena for short-ranged potentials will closely resemble the behavior of real systems is imprudent. Altogether new phenomena can emerge for moderately strong long-ranged potentials. Though these phenomena have been predicted on the basis of MFT, we expect that fluctuations will alter only details of the picture, as in the case of short-ranged potentials.

There are as yet no experiments that clearly test predictions near T_c. Recent work by Abeysuriya, Wu, and Frank[7] on mixtures of nitromethane and carbon disulfide suggests that this system might be useful in that regard. In an effort to control U_1 or, more generally, the short-ranged part of AS they employ chemical treatment (methylization) of the glass substrate. This appears to give rise to a change from wetting to nonwetting near T_c as a function of the degree of methylization. We note, however, that there is some controversy[7,8] over the nature of the long-ranged forces in the system.

We thank Carl Franck for informative discussions and correspondence concerning his experiments. This work was supported in part by National Science Foundation Grant No. DMR-84-04961.

[1]C. Ebner, W. F. Saam, and A. K. Sen, Phys. Rev. B **32**, 1558 (1985).

[2]C. Ebner and W. F. Saam, Phys. Rev. B **35**, 1822 (1987).

[3]M. P. Nightingale and J. O. Indekeu, Phys. Rev. B **32**, 3364 (1985); P. G. de Gennes, C. R. Acad. Sci. **297**, 9 (1983). See also V. Privman, J. Chem. Phys. **81**, 2463 (1984), where some informative mean-field calculations for a continuum model are carried out.

[4]H. Nakanishi and M. E. Fisher, Phys. Rev. Lett. **49**, 1565 (1982).

[5]The marginal-range real-world potential varies as $1/z^{2.45}$ (see Ref. 2). For longer-ranged potentials wetting transitions always occur, and always for $T < T_c$.

[6]Of course, for very strong long-ranged, attractive potentials, it is possible to eliminate nonwetting altogether. A $T=0$ argument shows that this occurs (for $U_1 > 0$) for $|U| > 12.01\ \varepsilon_\perp \nu_\perp$. Such unphysically strong potentials are not considered here.

[7]K. Abeysuriya, X.-L. Wu, and C. Frank, unpublished.

[8]R. F. Kayser, Phys. Rev. Lett. **56**, 1831 (1986), and unpublished work.